ACS APPLIED MATERIALS & INTERFACES

Research Article

www.acsami.org

Fluorescence and Piezoresistive Cantilever Sensing of Trinitrotoluene by an Upper-Rim Tetrabenzimidazole Conjugate of Calix[4]arene and Delineation of the Features of the Complex by Molecular Dynamics

Manoj Kandpal,[†,‡] Anil Kumar Bandela,[‡,§] Vijaya Kumar Hinge,[⊥] V. Ramgopal Rao,*[,†] and Chebrolu Pulla Rao*[,§,⊥]

[†]Centre of Excellence in Nanoelectronics, Department of Electrical Engineering, [§]Bioinorganic Laboratory, Department of Chemistry, and [⊥]Department of Biosciences and Bioengineering, Indian Institute of Technology Bombay, Powai, Mumbai 400076, India

Supporting Information

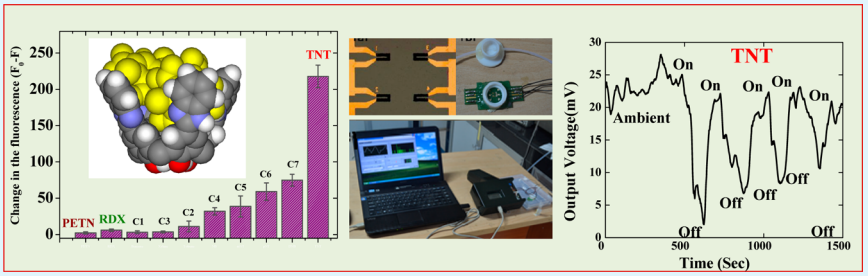

ABSTRACT: A new benzimidazole-functionalized calix[4]arene receptor (**R**) was synthesized and characterized. The receptor **R** shows better selectivity toward trinitrotoluene (TNT) compared to the other nitro explosives in solution, which also retains its effectiveness for solid-phase detection. The chemical interactions of the molecule with different nitro explosive analytes were studied by fluorescence spectroscopy and by a molecular dynamics approach. The molecular dynamics studies show a 1:3 complex between **R** and TNT, and hence high sensitivity was imparted by fluorescence studies. The detection of explosive vapors in ambient conditions was tested by using a sensitive coating layer of **R** on an SU-8/CB-based piezoresistive cantilever surface. The developed device showed large sensitivity toward TNT compared to cyclotrimethylenetrinitramine (RDX) and pentaerythritol tetranitrate (PETN) in the solid state at their respective vapor pressures at room temperature. The detection sensitivity of the device was estimated to be 35 mV for TNT at ambient conditions. Moreover, the sensor does not show a response when exposed to humidity. These results demonstrate that **R** can be used as one of the coating materials for a cantilever for the detection of TNT using piezoresistivity measurement. **R** can also detect the explosives in solution with high sensitivity and selectivity by fluorescence spectroscopy.

KEYWORDS: *upper-rim benzimidazole conjugate of calix[4]arene, fluorescence quenching, molecular dynamics, SU-8/CB cantilever, selective sensing of TNT*

INTRODUCTION

Real-time monitoring of explosives in the gas phase as well as in solution poses challenges to researchers owing to their extremely low vapor pressure and the presence of common interferences in the complex media.[1−6] Different types of organic molecular frameworks have been used as sensors for their explosive detection, where the detection is based on the induced physical and chemical changes that occur in the receptor upon interaction with the guest molecule.[1,4,7] While fluorescence spectroscopy has been an indispensible technique for sensing the analyte, a recent study of ours showed that a microcantilever can also be an efficient tool for sensing explosives having low vapor pressures.[5] The surface stress generated from interaction between the receptor and target molecule can lead to a deflection of the cantilever, which can be read out either externally by optical means or using internally by electrical means. Although the sensitivity issue can be addressed using cantilevers made up of a conductive SU-8 polymer and carbon black, the selectivity is still an important issue for the detection of explosives and this can be addressed by judiciously chosen receptor molecules possessing suitable chemical features. In the literature, microcantilevers have been used to detect explosives such as trinitrotoluene (TNT) and cyclotrimethylenetrinitramine (RDX) by using 4-mercaptobenzoic acid (4-MBA) and fluoro alcohol polysiloxane (SXFA) as detection coating layers.[8,9] The common problem with 4-MBA is its sensitivity toward humidity, while that of SXFA is in making a proper coating. Thus, there exists a need for the

Received: October 4, 2013
Accepted: December 2, 2013
Published: December 3, 2013

design of a molecular system that can exhibit high sensitivity and selectivity toward the molecules of explosives. Owing to the presence of a specific binding core and supramolecular architecture, calix[4]arene can act as a good receptor to impart selectivity to guest species when they are functionalized appropriately using suitable chemical moieties. Recently, calix[4]arene-based derivatives have been reported to detect TNT in a liquid as well as a vapor phase by fluorescence spectroscopy,[7,10] while the vapor-phase detection of trinitrobenzene has been demonstrated by using a calix[4]pyrrole-coated polyamide cantilever.[11] Therefore, in this paper, we report the synthesis and characterization of an upper-rim modification of calix[4]arene using the benzimidazole moiety and its utility as a receptor (**R**). In order to support the studies of the explosive molecules, fluorescence emission studies were also carried out with different nitro derivatives and the interactions were modeled by molecular dynamics (MD) methods. In addition, a protocol for the preparation of stable thin films of **R** over a SU-8 surface was established, and this was characterized by surface techniques, such as optical microscopy and contact angle. This was subsequently used for immobilizing the same on a cantilever surface to measure the deflection when the guest molecule interacts. On the basis of the fluorescence technique, **R** reported in this paper was found to be more sensitive toward TNT compared to other explosives, such as RDX and PETN, and the cantilever device made using **R** showed sensing through piezoresistive signals at ambient conditions.

EXPERIMENTAL SECTION

^{1}H and ^{13}C NMR spectra were measured on a 400 MHz NMR spectrometer. Mass spectrometry (MS) spectra were recorded on a Q-TOF instrument using the electrospray ionization (ESI) method. Fourier transform infrared (FTIR) spectra were recorded by the KBr pellet method. Fluorescence and absorption studies were carried out with a high-performance liquid chromatography grade solvent. All of the fluorescence studies were carried out in a 1 cm quartz cell and in all titrations, the concentration of **R** was kept constant at 10 μM [100 μL of dimethyl sulfoxide (DMSO) was used for dissolving **R**] in tetrahydrofuran (THF), while the concentrations of the guest species were varied. The concentration of the guest varies starting from 10 μM (to achieve 1:1 mole ratio) to 150 μM (to achieve 1:15 mole ratio). For atomic force microscopy (AFM) studies, 10^{-5} M concentrations of **R**, (**R** + TNT), and TNT solutions were used. Before drop casting, these solutions were sonicated for 10 min in order to avoid the formation of lumps. The same procedure has been followed for transmission electron microscopy (TEM) studies except that the concentration of **R** taken was 5×10^{-3} M.

Synthesis and Characterization of the Receptor Molecule R. The synthesis and characterization of the precursors P1, P2, and P3 are given in the Supporting Information (S1 and S2). To a mixture of P3 (0.2 g, 0.373 mmol) in methanol was added with stirring *o*-phenylenediamine (0.17 g, 1.512 mmol), and stirring was continued for 3 days. The product was allowed to settle, filtered, washed thoroughly with methanol, and dried under vacuum. Yield: 0.155 g, 64%. ^{1}H NMR (DMSO): δ 7.2 (s, 8H, Ar−H), 7.6 (s, 8H, Ar−H), 7.9 (s, 8H). 12.8 (br, 4H, NH). ^{13}C NMR (400 MHz, DMSO-d_6): δ 114.6, 118.1, 123.1, 127.8, 130.7, 131.1, 137, 137.4, 151.9, and 158.5. ESI-MS: m/z 445 (M/2), 100%, 889.6 $(M + 1)^+$. HRMS: 889.3270 (obsd), 889.3251 (calcd). FTIR (KBr phase): 3181 m, 2961 s, 2932 w, 1673 s, 1590 m, 1457 m, 1313 m, 1278 m, 1160 s, 1134 m, 994 s, 956 m cm^{-1} (S3 in the Supporting Information).

Computational Methodologies. The computational calculations carried out were of two types. The first one was optimization of the individual molecules/species by density functional theory (DFT), and the second one was MD simulation to obtain a complex of the explosive molecule or its control molecule with **R**. Thus, **R** along with TNT, PETN, nitrobenzene (C4), or dinitrobenzene (C7) was optimized using the *Gaussian G03* package.[12] In the case of **R**, the initial guest structure used for computational calculations was taken from the single-crystal X-ray diffraction data reported by us[13] by bringing the following modifications: (i) removal of the lower-rim ethylnapthalimide arms present at the 1 and 3 positions, followed by protonation of the phenolate oxygen atoms; (ii) removal of *tert*-butyl moieties present at the upper rim and the addition of benzimidazole moieties into that position. This initial structure has been optimized by going through a cascade process of PM3 → HF/STO-3G → HF/3-21G → HF/6-31G → B3LYP/3-21G → B3LYP/6-31G. The output obtained at every stage has been given as input for the next-higher level of calculations. TNT, PETN, C4, and C7 were modeled computationally using the *Gaussian G03* package at the B3LYP/6-31G level and were used for further studies.

The interactions present between **R** and the guest species were modeled by carrying out MD simulations under vacuum using the *Gromacs 4.0.5* package.[14] Vacuum simulations, which will require less computational time, were chosen to elucidate possible interactions between **R** and the guest molecules forming the inclusion complexes, and these were modeled. The simulations were carried out for 2 ns using the DFT-optimized structures, viz., {**R** + six copies of the guest species}, wherein all are randomly placed using an Accelrys DS visualizer. Force fields for **R** and the guest species were generated using the PRODRG2.5 server[15] and were included in the topology file. The charges for **R** and the guest species were calculated using the ChelpG[16] method using *Gaussian 03* software and were added in the same topology file. The total content of the system was then energy-minimized for ∼2000 steps with the steepest-descent method.[17] The entire system was treated under *NVT* conditions (T = 300 K), with the equation of motion being integrated by a leapfrog algorithm with a step size of 2 fs. At the time of carrying out the computations, **R** and the guest species were coupled separately to a V-rescale temperature bath. The V-rescale bath is stable enough to control fluctuations in the kinetic energy of **R** and the guest species separately.[32−34] The electrostatic interactions were calculated by using the particle-mesh Ewald summation method.[18] All of the bond lengths of **R** and the guest species were constrained using the LINCS algorithm.[19] The complexation energy was calculated using the formula $\Delta E_s = E_{\mathbf{R}:\text{guest}} - (E_{\mathbf{R}} + E_{\text{guest}})$.

Cantilever Fabrication. The cantilever was prepared using a five-mask process. Briefly, the silicon wafers (4−7 Ω·cm) were cleaned with a standard RCA cleaning process, and subsequently a 1-μm-thick thermal oxide layer was grown with a wet thermal oxidation process. A thin layer of SU-8 2002 (Microchem Corp., Newton, MA) of thickness 500 nm was spun over the oxide surface, and the cantilever layer was defined with optimized process parameters of prebaking at 70 °C for 3 min and 90 °C for 4 min. Patterns of cantilevers were defined on the spun SU-8 layer by exposing the wafer to UV light by using a Karl Suss MJB3 mask aligner followed by a postbaking step at similar heat cycles as those used for the prebaking process. A piezoresistive strain-sensitive SU-8/CB nanocomposite layer was prepared using CB nanoparticle dispersion in a SU-8 matrix that was spin-coated and patterned. Then a 20/200 nm Cr/Au layer was sputtered over the SU-8/CB nanocomposite layer and patterned to define the electrical contact. The encapsulation layer of SU-8-2002 of thickness 500 nm was spin-coated and patterned for passivation of the electrical pads. Lastly, the anchor for the devices was fabricated with a thick SU-8-2100 layer of thickness of around 150−200 μm, which was spin-coated and patterned. Cantilever structures were released from the substrate with removal of the sacrificial layer by using HF (7:1) and oxide wet chemistry.

Chip Immobilization and Interconnection Preparations. The microcantilever chip die was characterized for its resistance. The electrical resistance of the cantilevers was measured with the help of a Keithley 4200 source meter, and the resistance of the cantilevers was found to be in the range of 200−300 kΩ. The testing chip was prepared by mounting the cantilever over the printed circuit board (PCB), and electrical connections for the chip were prepared with a

contact path between the pad and existing contact leads of the PCB by using a conducting silver epoxy that was cured at 80 °C for 1 h. Gas-flow cells for these devices were created by enclosing the cantilever chip with a small Teflon chamber and sealed properly. For immobilization, the chip was coated with receptor molecule **R**. A total of 2 mg of the compound **R** was dissolved in 50 μL of DMSO, and thereafter it was diluted with 950 μL of chloroform. This solution was drop cast over the cantilever surface for immobilization of the receptor. The cantilever chip was then connected in a Wheatstone bridge configuration; the direct-current voltage was recorded with a ADS123X TI board, and changes in the voltage were recorded upon exposure to TNT and other explosive analytes.

RESULTS AND DISCUSSION

Synthesis, Characterization, and Molecular Architecture. The synthesis of the designed receptor molecule having upper-rim functionalization on calix[4]arene, **R**, is given in Scheme 1. **R** was synthesized via three steps starting from *p*-

Scheme 1[a]

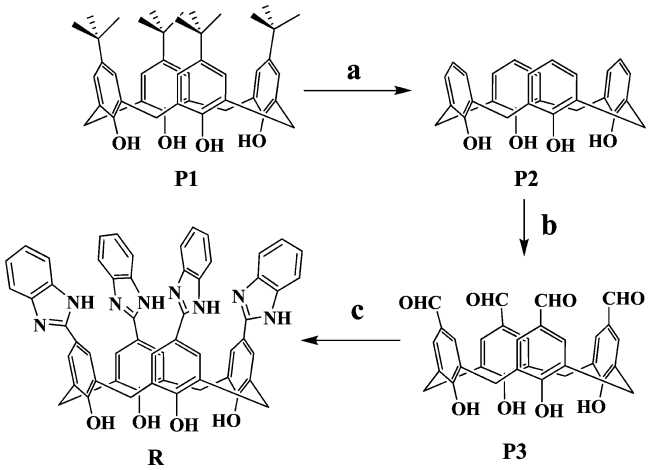

[a](a) $AlCl_3$, phenol, toluene, 50−60 °C, 2 h; (b) trifluoroacetic acid, hexamethylenetetraamine, 110 °C reflux, 24 h; (c) *o*-phenylenediamine, CH_3OH, 72 h.

tert-butylcalix[4]arene (P1) and its dealkylated form (P2) followed by the upper-rim tetraformyl functionalization (P3).[20,21] Finally, the receptor molecule **R** was synthesized by reacting P3 with *o*-phenylenediamine in methanol for 72 h. All of the molecules were characterized satisfactorily by ^1H and ^{13}C NMR, MS, and FTIR spectroscopy. The receptor **R** clearly provides an extended core upon conjugation with benzimidazole moieties at the para positions of the phenyl centers of the calix[4]arene platform, and this can be used as an interactive crevice for incoming guest species with selectivity. In addition, the lower-rim −OH moieties of **R** can be utilized to anchor the receptor onto the surface of silica, which can be further transferred onto the SU-8 surface.[22,23]

Absorption, Emission, and Selectivity. The absorption spectrum of **R** in a THF solvent exhibits two major characteristic bands, one at 220 nm and the other at 310 nm, arising from the arene and benzimidazole moieties, respectively (Figure 1a). When a 10 μM solution of **R** in THF is excited at 310 nm, it gives a broad emission band with additional contributions centered at 345, 360, and 395 nm. The intensity of the emission band was monitored as a function of increasing concentration of the guest. Different guest molecules were chosen as appropriate controls for TNT. The control molecules differ in their number and/or the position of the nitro group (Figure 1b). In addition, other common explosive molecules, such as RDX and PETN, were subjected to a similar study to assess the selectivity of **R**. Fluorescence titration spectra for the three explosives TNT, RDX, and PETN are shown in Figure 1c,d,e.

The fluorescence intensities were found to change based on the type of guest molecule employed for the titration, and hence the difference observed in the fluorescence intensity ($F_0 - F$) can be directly considered as a measure of the extent of interaction. Thus, the titration of **R** exhibited maximum quenching of the fluorescence intensity only when TNT was used, while the changes are minimal in the cases of C7, C6, C5, and C4 and are insignificant in the cases of other control molecules. The other explosive molecules, viz., RDX and PETN showed no appreciable change in the fluorescence intensity of **R**, providing selectivity to TNT over these. The results are shown as a bar diagram in Figure 1f for comparison. On the basis of fluorescence spectral studies, the minimium concentration of TNT that can be detected by **R** is 3.03 ± 0.05 μM. The binding constants were derived, and these were found to be in the range of 1000−30000 M^{-1} on going from C2 to TNT (Figure S4d in the Supporting Information). While the strongest one (TNT) has a K_a value of ∼30000 M^{-1}, those of the weaker ones are 1000−1500 M^{-1} for C2, C4, and C5. Thus, the binding of TNT is 20−30-fold stronger than that of these molecules.

In addition to the nitro compounds, fluorescence titrations were also carried out with some common aromatic molecules, such as benzene (C1), toluene (C2), and xylene (C3), to check whether these contribute to quenching, and no considerable quenching was observed (Figure S4a in the Supporting Information). These results show that the extent of quenching is maximum with TNT, which is ∼3-fold to those of C7 and C6, ∼4-fold to that of C5, and almost >35-fold to those of RDX, C1, C2, and C3 (Figure 1f). The fluorescence quenching observed in these titrations with **R** is attributed to an electron transfer from the excited benzimidazole arm to the incoming guest molecule that is complexed in the binding core through weak interactions (Figure S4b in the Supporting Information). Such excited-state electron transfer from the receptor to the TNT or other nitro compounds was also proposed in the literature.[7,24] Evidence for the weak interactions, such as hydrogen bonding and π···π, between benzimidazole moieties of **R** and TNT was derived from the MD simulation studies as reported in this paper.

Features of the Complexes of R by MD. To gain more insight into the interactions present between TNT and the receptor **R**, MD simulations were carried out at 2 ns. In order to understand its specificity toward the receptor, other explosive molecules, viz., RDX, PETN, and control molecules such as nitrobenzene (C4) and 1,3-dinitrobenzene (C7), were also subjected to similar MD studies. Stereoviews of these complexes are given in Figure S5 in the Supporting Information. The DFT-optimized structure of the receptor **R** shows the formation of a nice binding core enwrapped by the four benzimidazole moieties (Figure 2a). The structure of the complex species obtained at the end of 2 ns (Figure 2b) shows the incorporation of three TNT moieties, of which two are completely placed in the cavity while the third is projected out wherein the interacting benzimidazole moiety also tilts from the core. Each TNT interacts with each one of the benzimidazole moieties by exhibiting π···π interactions at distances of 3.7−4.0

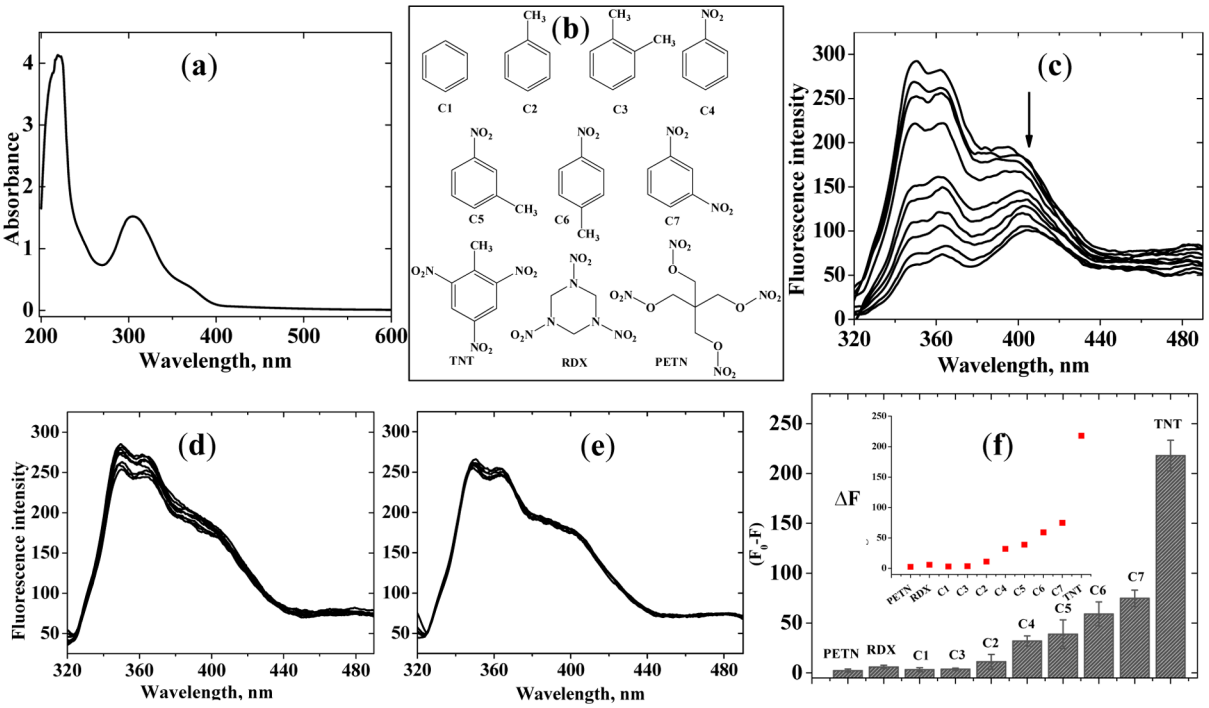

Figure 1. (a) Absorption spectrum of **R** measured in THF. (b) Guest molecules used in the present study. (c–e) Fluorescence spectra obtained during the titration of **R** with TNT, RDX, and PETN with increasing concentration to maintain requisite equivalents. (f) Histogram representing change in the the fluorescence intensity ($\Delta F = F_0 - F$) of **R** by various guest molecules taken at 15 equiv with respect to **R**. Inset: ΔF of **R** upon titration with various guest molecules when the **R**-to-guest mole ratio is maintained at 1:15. Error bars were obtained by repeating the titration experiments four times.

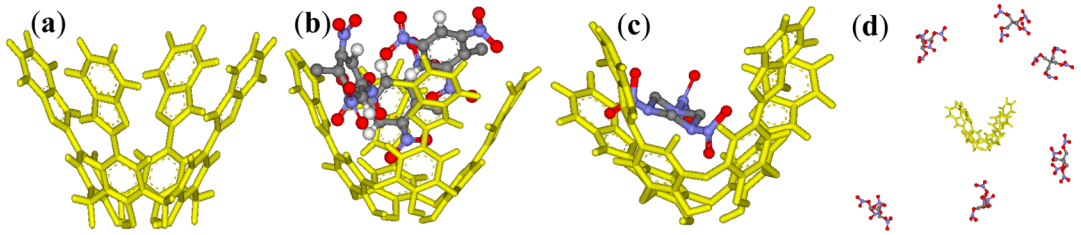

Figure 2. Structures obtained from a 2 ns MD simulation: (a) for simple **R**; (b) 1:3 complex of **R** with TNT; (c) 1:1 complex of **R** with RDX; (d) PETN with **R**, in which no complexation occurs.

Å. The structure of the complex reveals that there is no further possibility of having a fourth TNT incorporated without bringing further changes in the orientation of the benzimidazole moiety or moieties. This seems to suggest that, if the core present in the free receptor were to continue there even in the complex, more than two TNTs would not fit in. The TNTs were further stabilized through hydrogen-bonding interactions. One of the nitro groups of each of the TNTs is involved in hydrogen bonding either with the neighbor TNT or with the benzimidazole moiety. However, similar MD studies carried out using RDX show the incorporation of only one RDX sitting in the benzimidazole core of **R** in such a way that no more of RDX can be fitted, and this also brings tilt in the two consecutive benzimidazole moieties (Figure 2c). In the case of PETN, similar studies showed no incorporation of any of these molecules into the core and hence no complex formation (Figure 2d). Thus, among the three explosive molecules, TNT shows a large complexation energy of −64 kcal/mol, while RDX shows only −2.8 kcal/mol and PETN does not show any complex at all. However, in the case of RDX, because the complexation energy is higher than *kT*, complex formation is expected even at room temperature. The details of the corresponding stabilization energies are given in T6 in the Supporting Information. The observed ratio of the fluorescence intensity in the case of TNT, RDX, and PETN (70:2:1) is in accordance with the complexation energies derived from MD simulations. The 1:1 complex reported in the literature was that formed between one of the pyrene moieties of the lower-rim derivative and TNT; however, there is no clear-cut binding core formed in this,[10] unlike that present in our case. Thus, the TNT-capturing efficiency of **R** in the present case is 1:3, which is the highest in comparison to the previously reported 1:1 and 1:2 type complexes in the literature.[7,10,11] Further, the sensors reported in the literature do not possess a specific binding crevice to show any selectivity.

One of the control molecules, nitrobenzene (C4), perfectly fits into the core by tilting all four benzimidazole moieties to form one hydrogen bond each with the NO_2 group by acting as a N–H donor. Its further stabilization also comes from $\pi\cdots\pi$ interaction of C4 with the benzimidazole moiety at a distance of ∼3.5 Å. Even in the case of 1,3-dinitrobenzene (C7), only one molecule is trapped in the core (Figure S5 in the

dx.doi.org/10.1021/am404356v | *ACS Appl. Mater. Interfaces* 2013, 5, 13448–13456

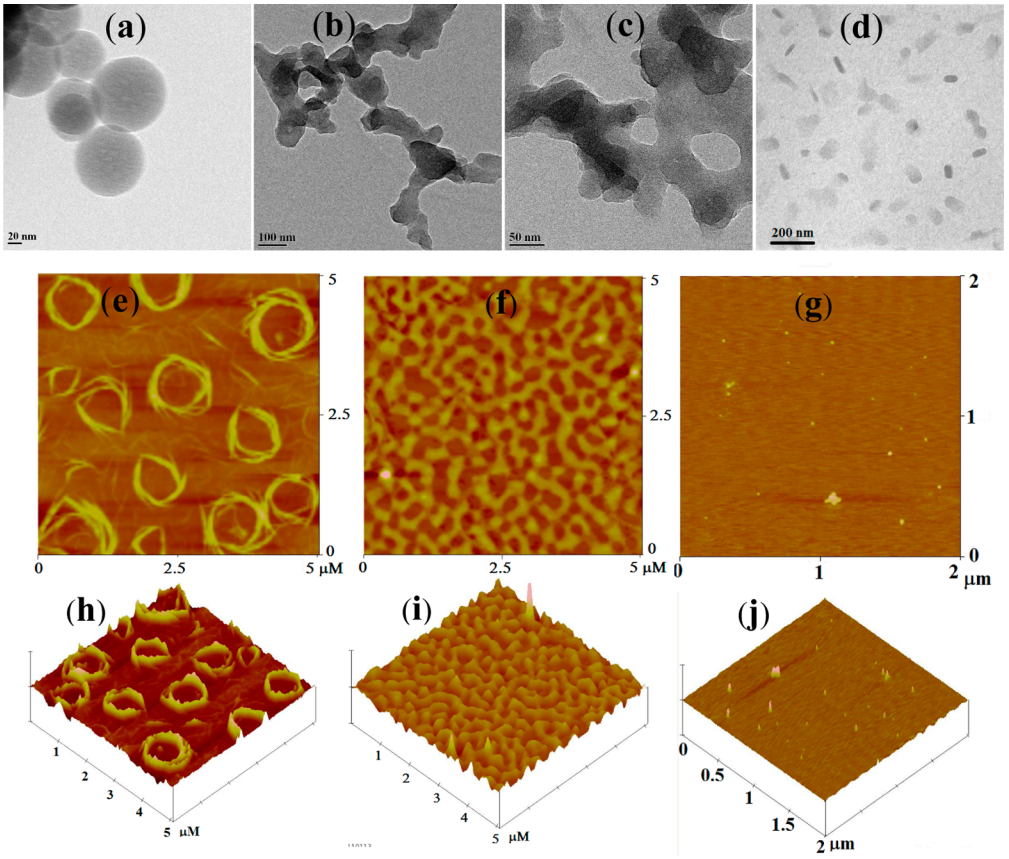

Figure 3. Top row: TEM micrographs for (a) the receptor **R**, (b and c) **R** + TNT, and (d) TNT. Middle and bottom rows: AFM micrographs for (e and h) the receptor **R**, (f and i) **R** + TNT, and (g and j) TNT .

Supporting Information), wherein the weak interactions are being extended between NO_2 and the lower rim and/or benzimidazole moieties. The lower stabilization energy observed in the case of C7 compared to C4 is attributable to the fact that C7 cannot be fitted into the crevice of **R** without making any conformational changes in the calixarene conjugate (Figure S5 in the Supporting Information). All of this implies that both the phenyl and NO_2 moieties of the guest species are important for interaction with the receptor possessing a benzimidazole-like moiety that has both a π component and a hydrogen-bonding site of nitrogen and their placement in the core. The complexation energies of all of these with **R** follow the trend TNT $\gg$ C4 > C7 > RDX, while PETN does not form any inclusion complex. Thus, MD simulations clearly support the conclusions derived based on the fluorescence titration that TNT can be more sensitively measured by **R** compared to the other explosive molecules, viz., RDX and PETN.

TNT-Induced Nanostructural Morphological Changes. The size and morphological features of **R** and its complex with TNT have been studied by TEM and AFM. Parts a–d of Figure 3 show TEM images of nanostructures of receptor **R** and its nanoaggregates with TNT as well as TNT alone as the control. The TEM study reveals that **R** exhibits spherical particles with diameter ranging from 50 to 80 nm. However, upon interaction with TNT, the spheriphicity is lost and a branched network like the nanostructures was observed that is attributable to the interactions present between **R** and TNT. However, TEM images taken for TNT show crystallite- or granule-type features, confirming that the nanostructural features observed for **R** + TNT are different from those of **R**. Interaction between the lower-rim benzimidazole conjugate of calix[4]arene and Hg^{2+} shows similar microstructural changes.[25] Many other conjugates of calix[4]arene and their interaction with metal ions or amino acids showed microscopic structural changes to differentiate the receptor from its complex with the guest species as a result of host–guest interactions, as reviewed recently.[26]

AFM carried out on a mica surface showed ring-like uniform nanostructures in the case of **R**, as can be seen from Figure 3e–j. The ring-like structures originate from aggregation of nanofibrils of **R**. In the AFM measured for **R** + TNT, the rings of fibrils observed in the case of **R** were broken and form extended structures, which are again uniform in nature and thus differ largely from the simple **R** resulting from the interactions present between **R** and TNT; however, TNT alone shows spherical-type nanofeatures. Thus, even the microstructural features observed in TEM and AFM clearly differentiate **R** from its complex of TNT and further support the presence of weak interactions existing between these species.

SU-8/CB Cantilever Fabrication and Immobilization of Thin Films of R and Surface Characterization. The effectiveness of receptor molecule **R** for its solid-phase detection of the vapors of explosive molecules, viz., TNT, RDX, and PETN, was tested on a sensitive piezoresistive SU-8/CB microcantilever platform. The credibility of a cantilever for the detection of lower concentrations of explosive vapors is its high sensitivity, which is due to the high surface-to-volume ratio. Further, the cantilever surface can be easily modified with organic molecules as receptors, where the guest species can interact, leading to measurable physical changes.[1−5] To

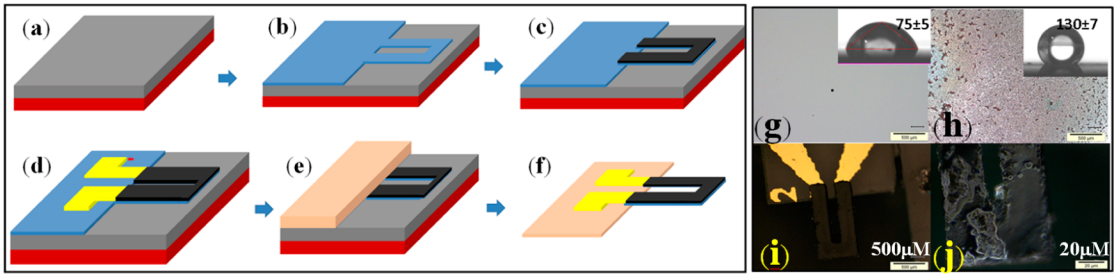

Figure 4. Fabrication process flow for SU-8/carbon black (CB) cantilevers. Color representation: red-brown layer, silicon wafer (4−7 Ω cm^2); gray layer, oxide layer (1 μm); blue layer, SU8 2002 layer (500 nm); black layer, carbon black (1.4 μm); yellow layer, Cr/Au layer (20/200 nm); cream color, SU8 100 layer (200 μm). (a) Thermally grown sacrificial oxide layer; (b) cantilevers defining the SU-8 layer; (c) SU-8/CB nanocomposite layer; (d) Cr/Au contact layer; (e) anchor layer, and (f) released device. Surface characterization results for the thin film of receptor **R** over the SU-8 surface: (g) uncoated; (h) coated. (i and j) Microscopy pictures of the uncoated and coated SU-8/CB cantilever surfaces, respectively.

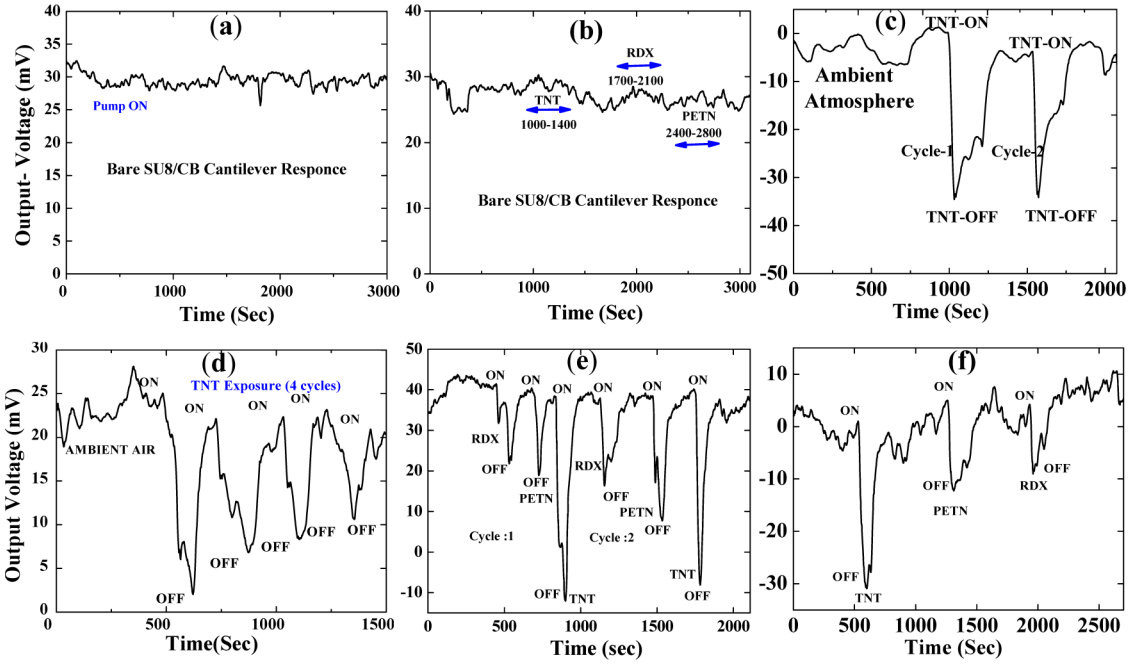

Figure 5. Response of the SU-8/CB cantilever toward TNT and other explosive analytes: (a) SU-8/CB bare cantilever ambient response; (b) SU-8/CB cantilever response to explosive molecules (without coating of **R**); (c) **R**-coated cantilever response for TNT as two on−off cycles; (d) **R**-coated cantilever response for TNT as four on−off cycles; (e) **R**-coated cantilever response for RDX, PETN, and TNT as two on−off cycles; (f) **R**-coated cantilever response for TNT, RDX, and PETN added to the system sequentially through on−off cycles.

determine the effectiveness of **R** in the solid state, SU-8/CB piezoresistive cantilevers of dimensions 250 × 50 × 3.2 μm^3 were used for experiments. Using the protocol adopted as reported by us earlier,[5] the chip was characterized to evaluate the deflection sensitivity, gauge factor, and surface sensitivity, by deflecting the microcantilever tip with a calibrated micromanipulator and simultaneously measuring the resistance with a Keithley 4200 sourcemeter. The deflection sensitivity, gauge factor, and surface stress sensitivity were extracted as 1.1 ppm nm^{-1}, 90, and 7.6 × 10^{-3} (N m^{-1})$^{-1}$, respectively. The process of flow for the fabrication of a SU-8/CB cantilever is shown in Figure 4a−f, and the working principle of the device is given in S8 in the Supporting Information. The released chip die was cleaned with isopropyl alcohol and subsequently rinsed with ultrapure deionized water (18.2 MΩ). Prior to immobilzation of **R** over the SU-8 cantilever, a thin film of **R** was prepared over the SU-8 surface, and its properties were investigated using optical microscopy and contact-angle measurements. A thin layer of **R** was prepared over the SU-8 surface by drop casting the solution of **R** (10^{-5} M) in a chloroform solution, where **R** was dissolved using a minimum quantity (50 μL) of DMSO. The layers of **R** deposited over the cantilever surface are thin films because the methodology used for the deposition is not expected to produce monolayer formation.

Immobilization of a thin film of **R** has been done similarly on the cantilever, and the film was characterized (Figure 4g−j). A significant improvement of the hydrophobic nature of SU-8 was observed with coating by **R**. The contact-angle measurements show an increase in the angle from 75 ± 5 to 130 ± 7°. This enhancement in the hydrophobic nature of the SU-8 surface can be attributed to the presence of hydrophobic moieties present in **R**. Microscopy pictures of a released die of the SU-8/CB cantilever and electrical contact preparation as well as chip characterizations are given in the Supporting Information (Figure S7).

Cantilever Testing. The experimental setup is equipped with a small pump that collects the sample vapors from the

explosive materials. The TNT vapors were generated from its powder, and ambient air was used as a carrier gas for measurements. The vapor pressure for the SU-8/CB cantilever experiments was maintained by keeping control over the variables such as the temperature and humidity. All of the sensing measurements with SU-8/CB cantilevers were performed at room temperature (25−30 °C) and a humidity of 60 (±10%) . At this temperature, the vapor pressures of TNT, RDX, and PETN are 9.9×10^{-4}, 6.3×10^{-7}, and 1.9×10^{-6} Pa, respectively, as reported in the literature.[27,28] In order to nullify the false response of the cantilever that arises because of the pump vibration and ambient moisture, the uncoated SU-8/CB cantilever responses were recorded for the first set of experiments. The pump was calibrated to a flow rate of 200 mL min^{-1} so that the cantilever response due to gas flow can be avoided, and ambient air was used as the sampling air for detection. As can be seen from Figure 5a, no characteristic peaks were observed corresponding to the vibrations of the pump. Similar experiments were also carried out with the uncoated SU-8/CB cantilever surface (S10 in the Supporting Information) to avoid any ambiguity of the cantilever response, which may be due to the interaction between trapped moisture on the SU-8/CB surface and the TNT analyte. Figure 5b shows the recorded cantilever response of the uncoated SU-8 surface to TNT and RDX. It can be clearly seen that no characteristic peaks were observed for two consecutive cycles of 400 s exposure of explosives. The drift of the signal that can be noticed in Figure 5b,c over a time period is known as Johnson noise, which is due to thermal fluctuations of charge carriers observed for piezoresistive detection-based sensors.[35] The variability in the noise level is different for each cantilever, and it depends on the dispersion quality and quantity of carbon black (CB) particles in the piezoresistive SU8/CB layer.[5]

After exclusion of the possibility of a false response due to SU-8 surface and pump vibrations, the experiments were carried out with a receptor **R**-coated SU-8/CB cantilever. The results of the SU-8/CB cantilever response after coating by **R** are shown in Figure 5c,d. It can be seen from Figure 5c that the cantilever was stable at room temperature and does not show any specific response for the first 1000 s. Subsequently, as the cantilever was exposed to TNT vapors, a significant change in the voltage was observed within the next 30−40 s. Once the vapors were turned off, the cantilever response came back to its normal state. The voltage respone ratio was almost 1:0.85 for the two cycles carried out, as given in Figure 5c. Similar trends were also observed when this experiment was repeated by using a fresh device and repeated four exposure cycles of TNT vapors (Figure 5d), wherein the response ratio was 1:0.8:0.75:0.67, and hence the error was ∼15−16% with respect to the average signal, exhibiting a rather consistent voltage response for TNT. The decrease in the response of the cantilever over the consecutive cycles (Figure 5d) was due to saturation of the surface with TNT vapors. Initially, when the device was fresh, more binding sites were available for analytes to react, leading to a greater change in the voltage, but as time progressed, the available binding sites for analyte decreased and hence there was a decrease in the signal during the next cycle.[5]

The rapid reversibility and fast relaxation of the SU-8/CB cantilever response confirms its sensitive detection of TNT with effective thin coatings of **R**. In the present work, we were able to show the repeatability of the detection signal by testing five sets of cantilever devices coated with **R**. The reproducibility was demonstrated (i) using TNT-crystalline and TNT-amorphous through on-off cycles followed by exposure to PETN at the end, (ii) using TNT followed by PETN followed by RDX as on−off cycles consecutively, (iii) by going through two cycles of TNT on−off, and (iv) by going through four consecutive cycles of TNT on−off. A comparison of the noises of each characterized device is given in T9 in the Supporting Information for five different devices. In all of these measurements, the TNT signals are always higher than the corresponding noise values.

In order to investigate the **R**-coated SU-8/CB cantilever response toward other common explosives, viz., RDX and PETN, the device was exposed to all three explosives one at a time in a series and the change in the voltage corresponding to each of these was recorded, as shown in Figure 5e,f. During the experiments, the temperature and humidty were fixed at 25 °C and 60 (±10)%, respectively. As shown in Figure 5f, the voltage responses of these cycles follow a 3:1.25:1 ratio for TNT, PETN, and RDX, suggesting that TNT is certainly sensed better by the cantilever system than RDX and PETN. Thus, the electrical response to TNT is almost 3 times greater than that to RDX. The possible reasons for such distinguishable patterns are the specific chemical affinity of TNT for **R** and also the higher vapor pressure observed for TNT over RDX and PETN at room temperature. A higher selectivity of the sensor toward these explosives is possible to obtain upon further optimization of the conditions of the thin film coating and other device parameters. It was also observed that the cantilever devices did not show any significant response when similar experiments were carried out with air as the control, while the explosive molecule produced a significant observed response (Figure 5c,d,e,f). In order to study the details of the selectivity of **R** with respect to the common interfering volatile species, a detailed study is indeed required, and such efforts are currently underway in our laboratory.

CONCLUSIONS AND CORRELATIONS

A new upper-rim benzimidazole conjugate of calix[4]arene (**R**) was synthesized and characterized and used in the present studies in order to improve the specificity of detection for TNT over the other explosives, such as RDX and PETN, by having a specific binding core. Recently, there are some noncalixarene receptors being studied for nitroaromatics that do not show any crevice or binding core like that being exhibited by calixarenes, although they form 1:1 complexes.[29−31] One of these indeed requires even modulation by the addition of a poisonous cyanide ion in 1 mM concentration.[31] In the present case, the fluorescence studies showed maximum quenching for TNT in comparison to the other explosive molecules as well as other nitro-based molecules of relevance when they were titrated against **R**. Thus, the comparison of the fluorescence response signal for TNT is far more superior than those of RDX and PETN, where their signals follow a ratio of 70:2:1 for TNT, RDX, and PETN, respectively. An understanding of the TNT interaction with **R** was studied with MD, which shows possible $\pi\cdots\pi$ interactions between the benzimidazole target moieties that form an aromatic binding core at the upper rim and TNT. The crevice of **R** shows effective interactions with three TNT molecules, while RDX has only one and PETN does not form a complex at all. This reflects the selectivity of **R** toward TNT by having an effective fit of three molecules in the crevice formed through the upper rim, over the other two explosive molecules. This can be clearly seen from the space-filling models given below for the optimized complexes (Figure 6a,b). The average

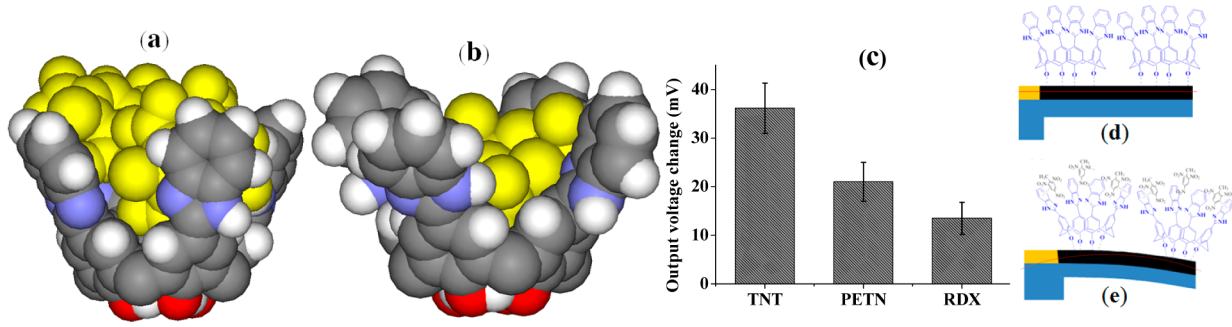

Figure 6. Space-filling model of the inclusion complexes of **R** with explosive molecules: (a) TNT (three molecules); (b) RDX (only one molecule). TNT and RDX are shown in yellow. (c) Histogram representing average changes in the voltage response of the cantilever with respect to TNT, RDX, and PETN (averaged over three devices). Conceptual diagrams depicting the response of the **R**-coated cantilever before (d) and after (e) exposure to TNT.

statistics obtained based on three devices corresponds to the observed signal of 36 mV for TNT, 21 mV for PETN, and 14 mV for RDX, as shown in the histogram given below (Figure 6c). The selectivity thus imparted by **R** is augmented by a very high sensitive fluorescence signal obtained for TNT over those of RDX and PETN using its upper-rim binding core. Both AFM and TEM studies showed clear-cut nanostructural features to differentiate **R** from its complex with TNT, based on the shape and size of the particles. The special structures formed in the microscopy support complex formation between **R** and TNT through the interactions mentioned in this paper.

The effectiveness of **R** in the solid state was tested by using it as a layer of coating on the SU-8/CB cantilevers. A fast and reversible change of the cantilever response observed within 30 s of TNT exposure is a result of the induced changes observed in the resistance of the cantilever, wherein the chemical interactions present between the receptor and guest species are translated into mechanical forces (Figure 6d,e). Thus, the voltage signal response is ~3 times greater for TNT compared to the other two explosive molecules, viz., RDX and PETN.

Therefore, the calix[4]arene-based receptor **R** reported in this paper is a highly promising molecular system for future applications particularly because of its specific and selective interaction with the guest explosive species in addition to the high sensitive piezoresistive property of the cantilever.

■ ASSOCIATED CONTENT

Supporting Information

Synthesis, fluorescence spectra, microscopy images, computational data, and cantilever data relevant to this paper but not given in the main manuscript. This material is available free of charge via the Internet at http://pubs.acs.org.

■ AUTHOR INFORMATION

Corresponding Authors

*E-mail: rrao@ee.iitb.ac.in.
*E-mail: cprao@iitb.ac.in.

Author Contributions

‡These authors have made equal contributions.

Notes

The authors declare no competing financial interest.

■ ACKNOWLEDGMENTS

C.P.R. thanks the DST, CSIR. and BRNS for financial support. A.K.B. and V.K.H. acknowledges the CSIR for their fellowships. V.R.R. acknowledges support from the Department of Information Technology, MCIT and DST, Government of India and the Nano-Sniff Technologies Pvt. Ltd., for providing their facility. We also thank Dr. Sheetal Patil and Priyanka Gupta for their help in the characterization and fabrication process.

■ REFERENCES

(1) Pinnaduwage, L. A.; Boiadjiev, V.; Hawk, J. E.; Thundat, T. *Appl. Phys. Lett.* **2003**, *83*, 1471−1473.
(2) Pinnaduwage, L. A.; Hawk, J. E.; Boiadjiev, V.; Yi, D.; Thundat, T. *Langmuir* **2003**, *19*, 7841−7844.
(3) Toal, S. J.; Trogler, W. C. *J. Mater. Chem.* **2006**, *16*, 2871−2883.
(4) Cerruti, M.; Jaworski, J.; Raorane, D.; Zueger, C.; Varadarajan, J.; Carraro, C.; Lee, S. W.; Maboudian, R.; Majumdar, A. *Anal. Chem.* **2009**, *81*, 4192−4199.
(5) Seena, V.; Fernandes, A.; Pant, P.; Mukherji, S.; Rao, V. R. *Nanotechnology* **2011**, *22*, 295501−295512.
(6) Grate, J. W. *Chem. Rev.* **2008**, *108*, 726−745.
(7) Costa, A. I; Prata, J. V. *Sens. Actuators, B* **2012**, *161*, 251−260.
(8) Mcgill, R. A.; Mlsna, T. E.; Chung, R.; Nguyen, V. K.; Stepnowski, J. *Sens. Actuators, B* **2000**, *65*, 5−9.
(9) Raorane, D.; Lim, S. -H.; Majumdar, A. *Nano Lett.* **2008**, *8*, 2229−2235.
(10) Lee, Y. H.; Liu, H.; Lee, J. Y.; Kim, S. H.; Kim, S. K.; Sessler, J. L.; Kim, Y.; Kim, J. S. *Chem.—Eur. J.* **2010**, *16*, 5895−5901.
(11) Zhu, W.; Park, J. S.; Sessler, J. L.; Gaitas, A. *Appl. Phys. Lett.* **2011**, *98*, 123501−123503.
(12) Frisch, M. J. *Gaussian 03*, revision C.02; Gaussian, Inc.: Wallingford, CT, 2004. See the Supporting Information, S11).
(13) Bandela, A.; Chinta, J. P.; Hinge, V. K.; Dikundwar, A.; Guru Row, T. N.; Rao, C. P. *J. Org. Chem.* **2011**, *76*, 1742−1750.
(14) Hess, B.; Kutzner, C.; van der Spoel, D.; Lindahl, E. *J. Chem. Theory Comput.* **2008**, *4*, 435−447.
(15) Schuettelkopf, W.; van Aalten, D. M. F. *Acta Crystallogr.* **2004**, *D60*, 1355−1363.
(16) Brenneman, C. M.; Wiberg, K. B. *J. Comput. Chem.* **1990**, *11*, 361−373.
(17) Deift, P.; Zhou, X. *Ann. Math.* **1993**, *137*, 295−368.
(18) Darden, T.; York, D.; Pedersen, L. *J. Chem. Phys.* **1993**, *98*, 10089−10092.
(19) Hess, B.; Bekker, H.; Berendsen, H. J. C.; Fraaije, M. J. G. E. *J. Comput. Chem.* **1997**, *18*, 1463−1472.
(20) Gutsche, C. D.; Levine, J. A.; Sujeeth, P. K. *J. Org. Chem.* **1982**, *50*, 5802−5806.
(21) Casnati, A.; Sartori, A.; Pirondini, L.; Bonetti, F.; Pelizzi, N.; Sansone, F.; Ugozzoli, F.; Ungaro, R. *Supramol. Chem.* **2006**, *18*, 199−218.
(22) Aswal, D. K.; Lenfant, S.; Guerin, D.; Yakhmi, J. V.; Vuillaume, D. *Anal. Chim. Acta* **2006**, *568*, 84−108.

(23) Walther, F.; Drobek, T.; Gigler, A. M.; Hennemeyer, M.; Kaiser, M.; Herberg, H.; Shimitsu, T.; Morfill, G. E.; Stark, R. W. *Surf. Interface Anal.* **2010**, *42*, 1735−1744.
(24) Venkatramaiah, N.; Kumar, S.; Patil, S. *Chem. Commun.* **2012**, *48*, 5007−5009.
(25) Joseph, R.; Ramanujam, B.; Acharya, A.; Khutia, A.; Rao, C. P. *J. Org. Chem.* **2008**, *73*, 5745−5758.
(26) Acharya, A.; Samanta, K.; Rao, C. P. *Coord. Chem. Rev.* **2012**, *256*, 2096−2125.
(27) Dionne, B. C.; Rounbehler, D. P.; Achter, E. K.; Hobbes, J. R.; Fine, D. H. *J. Energy Mater.* **1986**, *4*, 447−472.
(28) Marshall, M.; Oxley, J. C. In *Aspects of Explosives Detection*, 1st ed.; Marshall, M., Oxley, J. C., Eds.; Elsevier: Amsterdam, The Netherlands, 2009; pp 1−10.
(29) Kumar, S.; Venkatramaiah, N.; Patil, S. *J. Phys. Chem. C* **2013**, *117*, 7236−7245.
(30) Shanmugaraju, S.; Jadhav, H.; Karhik, R.; Mukherjee, P. S. *RSC Adv.* **2013**, *3*, 4940−4950.
(31) Bhalla, V.; Pramanik, S.; Kumar, M. *Chem. Commun.* **2013**, *49*, 895−897.
(32) Song, C.; Weichbrodt, C.; Salnikovc, S. E.; Dynowskid, M.; Forsberga, B. O.; Bechingerc, B.; Steinemb, C.; Groota, B. L.; de Zachariae, U.; Zeth, K. *Proc. Natl. Acad. Sci. U. S. A.* **2013**, *110*, 4586−4591.
(33) Shukla, R. T.; Sasidhar, Y. U. *Phys. Chem. Chem. Phys.* **2013**, *15*, 18571−18583.
(34) Mukherjee, K.; Pandey, D. M. *Bioinformation* **2012**, *8*, 881−885.
(35) Harley, J. A.; Kenny, T. W. *J. Microelectromech. Syst.* **2000**, *9*, 226−235.